ISMCR 2018 - 21th International Symposium on Measurement and Control in Robotics
26-28 September 2018 - International CBRNE Institute, MONS, Belgium
ROBOTICS FOR THE CHANGING WORLD

An Active Beacon-Based Tracking System To Be Used For Mobile Robot Convoying

S Goll[1,2] and E Zakharova[1,2]
[1]Department of Information-Measuring and Biomedical Engineering, Ryazan State Radio Engineering University (RSREU), Gagarin Street, 59/1, Ryazan, RU
[2]LLC KB Avrora, Skomoroshinskaja Street 9, of.3, Ryazan, RU

Abstract. The paper is focused on the mobile robot convoying along the path travelled by some leader carrying the active ultrasonic beacon. The robot is equipped with the three-dimensional receiver array in order to receive both the ultrasonic wave and the RF wave marking the beginning the of the measurement cycle. To increase measurement reliability each receiver contains two independent measurement channels with the automatic gain control. The distance measurements are preprocessed to remove identify the artifacts and either remove them or substitute with the interpolated value. To estimate the position of the beacon in the robot's local coordinate system several methods are used including least squares method with the subsequent exponential smoothing, linear Kalman Filter, Rauch-Tung-Striebel smoother, Extended Kalman Filter, Unscented Kalman Filter and the Particle Filter. The experiments were made in order to estimate the estimation method preferable for the leader's path following.

1. Introduction

The convoying scenario is one of the most important tasks for the modern robotics. A mobile robot autonomously following a leader can be widely used in such areas as agriculture, transportation and military. Many well-known international trials, such as ELROB, include this scenario either as an independent one or as a part of a more complex scenario.

The scenario is focused on the mobile robot autonomously following some leader who can be either a human operator or another vehicle, autonomous or remote controlled. To detect the leader different systems can be used, including GNSS systems [1, 2] video cameras [3, 4], infrared cameras [5], lidars [6], radars and ultrasonic rangefinders [7, 8]. The nature of these systems, however, can impose various restrictions on the conditions of their use. GNSS systems perform poorly in the urban areas and inside of the buildings. Lidars and radars can be used to measure distance between the vehicle and the surrounding objects, but it is a non-trivial task to detect the leader based on range data. Cameras, both video and infrared, can help with leader detection, but depend greatly on the environmental conditions. Moreover, if the obstacle appears between the leader and the robot the accuracy of their relative positions estimate can be severely decreased.

The mathematical methods used for localization, obstacle detection and occupancy grid mapping are not reliable enough to build a robust convoying system. Such methods usually require the redundant sensor data of different nature. The leader detection suffers from the same restrains and, to make things even more difficult, the rough weather conditions, dense vegetation, smoke and other factors should also be considered.

2. The approach

In this paper we propose an ultrasonic-based leader detection system which includes an active beacon carried by the leader and a set of N ultrasonic receivers mounted on the convoyed robot (figure 1).

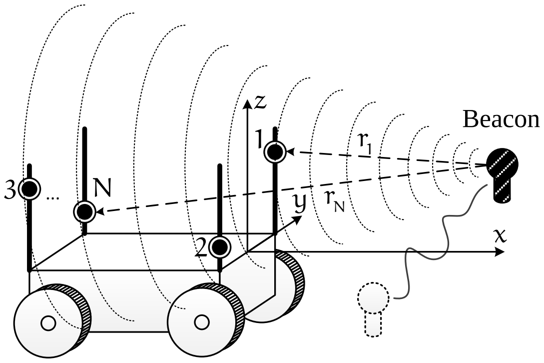

a


b

Figure 1. a – active beacon and the receiver array mounted on the mobile robot, b – convoying scenario with the two robots.

The active beacon transmits the ultrasonic waves with the constant time intervals between the waves. At the same time as the ultrasonic wave is sent the radio-frequency wave marking the beginning of the measurement cycle is also transmitted. For the each of the N receivers the time interval between the moment of radio-frequency wave and ultrasonic wave arrivals is measured according to the Time-of-Flight principle. These intervals are proportional to the distances between the beacon and the respective receivers and can be calculated as $r_n = c\tau_n$, $n = 1,\dots,N$, where c is the speed of the ultrasound in the air, τ_n is the time interval measured for the n th receiver.

To estimate the beacon's coordinates in the robot's local coordinate system the system of N nonlinear equations is solved.

$$r_n^2 = (x^m - x_n)^2 + (y^m - y_n)^2 + (z^m - z_n)^2,\ n = 1,\dots,N, \quad (1)$$

where $\vec{u} = \begin{bmatrix} x^m & y^m & z^m \end{bmatrix}^T$ is a vector containing coordinates of the beacon and the $\begin{bmatrix} x_n & y_n & z_n \end{bmatrix}^T$ are the coordinates of the n th receiver in the convoyed robot's local coordinate system.

During the system operation an obstacle can cause the line-of-sight loss between one or several receivers and the beacon. Moreover, the ultrasonic wave can be reflected by the surrounding objects causing the multipath propagation problem. For these reasons acquired measurements can contain artifact distances r_n (figure 2a) which are identified using the threshold constant ρ. The distance measurement $r_{n,k}$ is considered an artifact if the following condition is met

$$\left| r_{n,k} - r_{n,k-1} \right| > \rho, \quad (2)$$

where ρ is an adjustable threshold constant, k – consequent measurement number.

If the artifact is detected, the linear least square extrapolation is used to calculate the substitute estimate based on the last W estimates $\left\{ r_{n,k-1},\dots,r_{n,k-W} \right\}$.

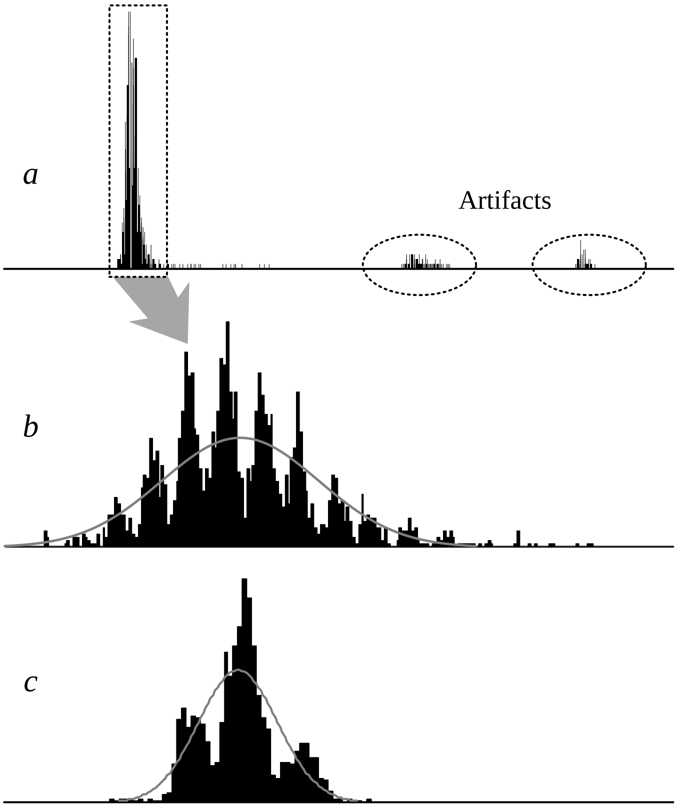

Figure 2. Histogram of centered values for the single receiver's measurements:
a – measurement series containing artifacts,
b – 11 meter distance between the beacon and the receiver,
c – 3 meter distance between the beacon and the receiver.

If the series of M artifacts is detected in the receiver's measurements or the substitute estimate cannot be calculated due to the unreliable measurements present in the last W estimates, the corresponding equations are excluded from the system (3). When the reliable measurements (i.e., the condition (2) is not met for the two consecutive measurements) arrive the receiver is included back in the system (3) and the artifact removal procedure becomes applicable again. The system must contain at least three reliable measurements from different receivers to calculate the beacon's position estimate $\vec{u}$. If there are not enough reliable measurements available the robot stops until the beacon's position can be calculated again.

To make more robust measurements each receiver contains two independent measurement channels with partly overlapping beam patterns and automatic gain control. If both channels succeeded at the distance measurement at some moment of time k, then the average value is used as a resulting measurement. If one of the channels failed to provide a measurement then the over channel's measurement is used as a resulting measurement.

3. Position estimation

Many of the effective estimation methods are based on the linear models and use normally distributed values. The figures 2b and 2c show the histograms of centered values for the measured distances r_n between the beacon and the n^{th} receiver with the beacon positioned along the axis of the receiver's beam pattern at the distance of 11 and 3 meters accordingly. Clearly, the histograms are multimodal with the constant distances $c \cdot \Delta\tau$ between the modes, where $\Delta\tau$ is the period of ultrasound.

Since the envelope's shape can be approximated with the Gaussian, we can assume that the distances r_n are distributed normally with the variance depending on the beacon's position. However, if we assume that the $\vec{u}$ values are normally distributed as well, then the r_n^2, as it appears in the (1), complies with the single-sided exponential distribution (figure 3). This means that distances r_n are not distributed normally.

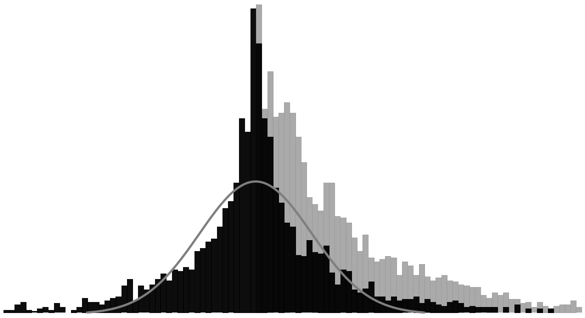

Figure 3. Distribution histograms for the r_n^2 (grey columns) and the g_l (black columns).

We can use linear combination of the equations to transform the nonlinear equations of (1) into the linear ones. For the each pair of receivers the difference of the squared distances to the beacon is calculated as follows
$r_i^2 - r_j^2 = (x^m - x_i)^2 + (y^m - y_i)^2 + (z^m - z_i)^2 - (x^m - x_j)^2 + (y^m - y_j)^2 + (z^m - z_j)^2$, where $i, j = 1, \ldots, N$, $i \neq j$, C_N^2 – binomial factor, $L = C_N^2$ – number of receiver combinations.

As a result, the system (1) can be written in the form of the linear system

$$B\vec{u} = \vec{g}, \qquad (3)$$

where B – system matrix with the L rows containing $\left[2(x_j - x_i) \quad 2(y_j - y_i) \quad 2(z_j - z_i)\right]$, $\vec{g}$ – column vector of L constant terms $\left(r_i^2 - r_j^2 + x_j^2 - x_i^2 + y_j^2 - y_i^2 + z_j^2 - z_i^2\right)$, $i, j = 1, \ldots, N$, $i \neq j$.

Generally, the system (3) is inconsistent due to the measurement noise. Hence, to estimate the position of the beacon the least squares method can be used $\vec{u} = \left(B^T B\right)^{-1} B^T \vec{g}$.

If $\vec{u}$ is distributed normally, then g_l, $l = 1, \ldots, L$ in (3) complies with the two-sided exponential distribution as shown in the figure 3 with the black-colored columns. This distribution can be approximated by the Gaussian more accurately than the single-sided one, increasing the accuracy of the estimate obtained with most of the effective methods.

To compute the estimate $\vec{u}$ of the beacon's position different methods can be used, therefore several estimates were computed in the course of research. Since all the methods are well-known and widely used it seem unnecessary to describe them. For that reason only the implementation details are provided for the each method.

During the research the receiver array of $N = 4$ receivers was used, therefore, the system (3) contains $L = C_4^2 = 6$ equations.

3.1. Least squares method with the exponential smoothing

$$\vec{u}_k^s = \alpha\vec{u}_k + \left(1 - \alpha\right)\vec{u}_{k-1}^s,\ \alpha \in \left(0;1\right), \qquad (4)$$

where α is the adjustable smoothing factor.

3.2. Kalman Filter with the non-stationary measurement noise matrix

The overall filter design is done according to [9]. Still, several implementation details should be clarified. According to (3) the stochastic system model can be described as follows

$$\begin{cases} \vec{x}_{k+1} = A\vec{x}_k + \vec{\xi}_k, \\ \vec{g}_k = C\vec{x}_k + \vec{\eta}_k, \end{cases} \tag{5}$$

$\vec{x}_k = \begin{bmatrix} x_k^m & y_k^m & z_k^m & v_k^x & v_k^y & v_k^z \end{bmatrix}^T$ – state vector containing beacon's coordinates and velocity components; $A = \begin{bmatrix} 1 & 0 & 0 & \Delta t & 0 & 0 \\ 0 & 1 & 0 & 0 & \Delta t & 0 \\ 0 & 0 & 1 & 0 & 0 & \Delta t \\ 0 & 0 & 0 & 1 & 0 & 0 \\ 0 & 0 & 0 & 0 & 1 & 0 \\ 0 & 0 & 0 & 0 & 0 & 1 \end{bmatrix}$ – stationary transition matrix of the dynamic model, where Δt – time interval between the consecutive measurements; $\vec{g}_k = \begin{bmatrix} g_{1,k} & \dots & g_{L,k} \end{bmatrix}^T$ – measurement vector; C – stationary measurement model with L rows $\begin{bmatrix} 2(x_j - x_i) & 2(y_j - y_i) & 2(z_j - z_i) & 0 & 0 & 0 \end{bmatrix}$, $i, j = 1, \dots, N$, $i \neq j$; $\vec{\xi}_k = \begin{bmatrix} 0 & 0 & 0 & a_k^x & a_k^y & a_k^z \end{bmatrix}$ – process noise, $\vec{\xi}_k \sim \mathbb{N}\left(\vec{\xi}_k \middle| \vec{0}, Q\right)$, $Q = diag\left(0, 0, 0, \sigma_a^2, \sigma_a^2, \sigma_a^2\right)$ – stationary process noise covariance matrix; $\vec{\eta}_k$ – observation noise vector, $\vec{\eta}_k \sim \mathbb{N}\left(\vec{\eta}_k \middle| \vec{0}, R_k\right)$, R_k – non-stationary measurement noise covariance matrix.

To estimate the measurement noise covariance [10] we assume that $R_k = E\left[\vec{s}_k \vec{s}_k^T\right] + CP_kC^T$, where $\vec{s}_k$ – measurement residual (also called innovation), when $R_k = \begin{cases} R_0, & k < D \\ \frac{1}{D}\sum_{d=k-D}^{k} \vec{s}_d \vec{s}_d^T + CP_kC^T, & k \geq D \end{cases}$, D – the estimation window size.

The initial state vector is assumed to be $\vec{x}_0 = \begin{bmatrix} x_0^m & y_0^m & z_0^m & 0 & 0 & 0 \end{bmatrix}^T$, where $\begin{bmatrix} x_0^m & y_0^m & z_0^m \end{bmatrix}^T = (B^TB)^{-1}B^T\vec{g}_0$. The posteriori error covariance matrix and the measurement noise covariance matrix are written as $P_0 = diag\left(\sigma_u^2, \sigma_u^2, \sigma_u^2, \sigma_v^2, \sigma_v^2, \sigma_v^2\right)$ and $R_0 = diag\left(\underbrace{\sigma_g^2, \cdots, \sigma_g^2}_{L}\right)$ respectively.

3.3. Rauch-Tung-Striebel smoother

The sequence of beacon's state estimates $\left\{\vec{x}_k, \vec{x}_{k-1}, \dots, \vec{x}_{k-T}\right\}$ can be used to set the desired path for the mobile robot. If the corresponding covariance matrices $\left\{P_k, P_{k-1}, \dots, P_{k-T}\right\}$ are also known, then this path-to-be can be smoothed using the Rauch-Tung-Striebel smoother. The estimate and covariance sequences are rewritten as $\left\{\vec{x}_T, \vec{x}_{T-1}, \dots, \vec{x}_0\right\}$ and $\left\{P_T, P_{T-1}, \dots, P_0\right\}$ accordingly. The initial smoothed estimate is $\vec{x}_T^s = \vec{x}_T$ with the covariance $P_T^s = P_T$. Then the smoother is applied from the last time step to the first (i.e., $t = T-1, \dots, 0$) according to the description given in [9]

3.4. Extended Kalman Filter

According to (1) the stochastic system model can be described as follows:

$$\begin{cases} \vec{x}_{k+1} = A\vec{x}_k + \vec{\xi}_k, \\ \vec{r}_k = \vec{h}\left(\vec{x}_k\right) + \vec{\eta}_k, \end{cases} \tag{6}$$

$\vec{h}\left(\vec{x}_k\right)$ – vector-valued function containing N elements $\sqrt{(x_k^m - x_n)^2 + (y_k^m - y_n)^2 + (z_k^m - z_n)^2}$, $n = 1,\dots,N$, $\vec{r}_k = \begin{bmatrix} r_{1,k} & \dots & r_{N,k} \end{bmatrix}^T$ – measurement vector. The measurement noise covariance matrix $R_k = \begin{cases} R_0, & k < D \\ \frac{1}{D}\sum_{d=k-D}^{k} \vec{s}_d\vec{s}_d^T + H_k P_k H_k^T, & k \geq D \end{cases}$ is non-stationary with the initial value of $R_0 = diag\Big(\underbrace{\sigma_r^2,\cdots,\sigma_r^2}_{N}\Big)$, H_k – Jacobian matrix. As for the other parameters used in (6) , they are the same as for the linear filter described above. The implementation is done according to the [9].

3.5. Unscented Kalman Filter

The problem-dependent filter parameters are the same as for the Extended Kalman Filter and were described above. The measurement noise covariance matrix $R_k = \begin{cases} R_0, & k < D \\ \frac{1}{D}\sum_{d=k-D}^{k} \vec{s}_d\vec{s}_d^T + \Upsilon_k W \Upsilon_k^T, & k \geq D \end{cases}$ is non-stationary with the initial value of $R_0 = diag\Big(\underbrace{\sigma_r^2,\cdots,\sigma_r^2}_{N}\Big)$, $\Upsilon_k = \vec{h}(X_k)$, X_k – array of sigma points, W – matrix of weights. The filter implementation complies with the [9].

3.6. Particle Filter

To describe the beacon's position the following state vector $\vec{x} = \begin{bmatrix} x^m & y^m & z^m & v^x & v^y & v^z \end{bmatrix}^T$ is used, where $\vec{x} \sim \mathbb{N}\left(\vec{x} \,\middle|\, \vec{x}_0, \Sigma\right)$. The initial estimate is $\vec{x}_0 = \begin{bmatrix} x_0^m & y_0^m & z_0^m & 0 & 0 & 0 \end{bmatrix}^T$, where $\vec{u}_0 = \begin{bmatrix} x_0^m & y_0^m & z_0^m \end{bmatrix}^T = \left(B^T B\right)^{-1} B^T \vec{g}_0$, $\Sigma = diag\left(\sigma_u^2, \sigma_u^2, \sigma_u^2, \sigma_v^2, \sigma_v^2, \sigma_v^2\right)$.

Based on the distribution $\mathbb{N}\left(\vec{x} \,\middle|\, \vec{x}_0, \Sigma\right)$ the set of particles X_0 is generated. For the each particle $\vec{x}_{j,k}$ the weight $w_{j,0} = 1/J$ is set, with the sum of weights $w_\Sigma = \sum_{j=1}^{J} w_{j,0} = 1$, $j = 1,\dots,J$.

The prediction step is done according to $X_k = AX_{k-1}$. During the update step for the each particle $\vec{x}_{j,k}$ distances $\hat{r}_{n,j,k}^2$ to the each of the receivers are calculated according to the equation

$$\hat{r}_{n,j,k}^2 = \left(x_{j,k}^m - x_n\right)^2 + \left(y_{j,k}^m - y_n\right)^2 + \left(z_{j,k}^m - z_n\right)^2, \; n = 1,\dots,N, \; j = 1,\dots,J$$

We assume that distances between the n th receiver and the beacon are distributed normally $p\left(\hat{r}_{n,j,k}^2\right) = \mathbb{N}\left(\hat{r}_{n,j,k}^2 \,\middle|\, r_{n,j,k}^2, \sigma\right)$, where $r_{n,j,k}^2$ – measurement of n th receiver. Weight for each particle calculate according to the equation $w_{j,k} = p\left(\hat{r}_{1,j,k}^2\right) \cdot \ldots \cdot p\left(\hat{r}_{N,j,k}^2\right)$.

Then the particles with the weighs less than β are removed from the set and the weights are normalized according to the equation $\vec{w}_k = \frac{1}{\sum_{j=1}^{\Omega} w_{j,k}} \vec{w}_k$, where Ω is the size of the new particle set.

The state vector is computed as $\vec{x}_k = \sum_{j=1}^{\Omega} w_{j,k} \vec{x}_{j,k}$. After that new particles are added to the set according to the normal distribution $\mathbb{N}\left(\vec{x} \middle| \vec{x}_k, \Sigma_x\right)$ up to the number J. Then the next prediction step is executed.

4. Results

During the experiment the mobile robot equipped with the active beacon moved along the 4.6×7 m rectangular path (figure 4). The array of $N = 4$ receivers was statically placed outside of that path with the center at (0;0).

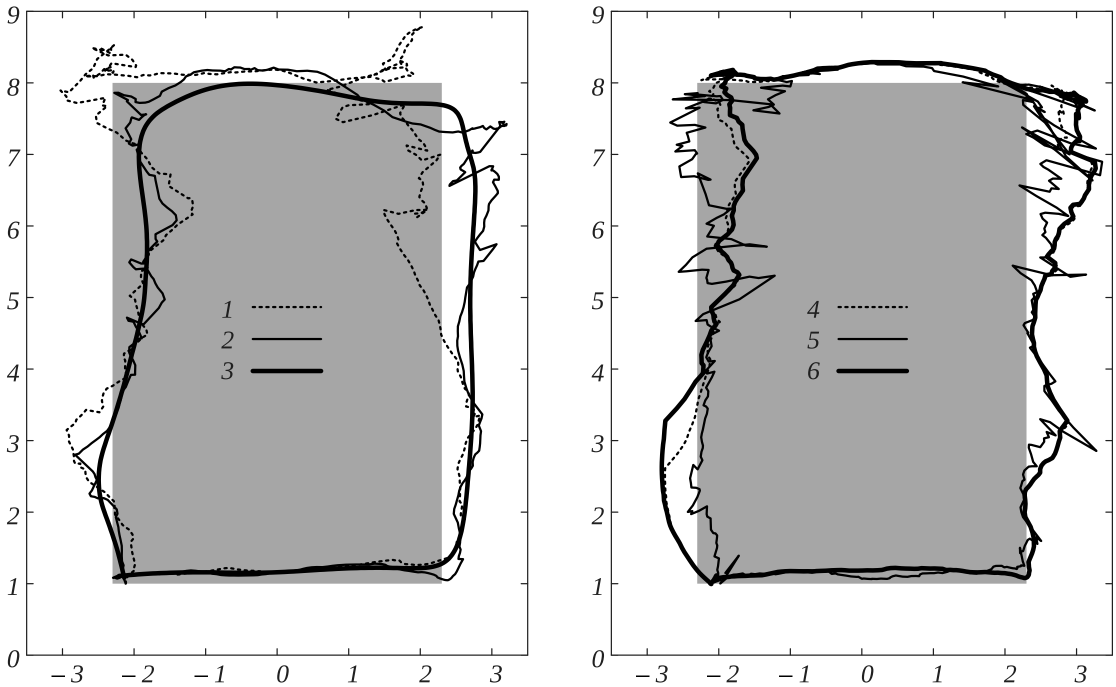

Figure 4. Beacon's path estimates: 1 – least squares method with the exponential smoothing, 2 – Kalman Filter, 3 – Kalman Filter with Rauch-Tung-Striebel smoother, 4 – Unscented Kalman Filter, 5 – Particle Filter, 6 – Extended Kalman Filter.

For the each beacon's position a total of 6 estimates were computed using the methods described above. To make a comparison between the performances of different methods the average of root mean square errors (RMSE) was used. The results are shown in the table 1. Clearly, the Rauch-Tung-Striebel smoother is preferable to estimate the path made by the active beacon which a mobile robot has to follow.

Table 1. A comparison between different methods using root mean square errors (RMSE)

	RMSE(x^m), m	**RMSE(y^m), m**
ES	0.4617	0.5737
KF	0.2910	0.5433
RTS	0.2230	0.4223

EKF	0.2478	0.4987
UKF	0.2305	0.4349
PF	0.1918	0.4958

5. References

[1] Spencer M, Jones D, Kraehling M and Stol K 2007 Trajectory based autonomous vehicle following using a robotic driver, *Australasian conference on robotics and automation, Brisbane: Australian Robotics and Automation Association*, Sydney, Australia, pp. 1-10.

[2] Wong N, Stol K A, Chambers C and Halkyard R 2009 Autonomous vehicle following using a robotic driver, *IEEE 15th international conference on mechatronics and machine vision in practice*, Auckland, New Zealan, 2-4 December 2008, pp.115-120.

[3] Changchen Z, Weihai C, Zhiwen Z and Jingmeng L 2013 An RGBD data based vehicle detection algorithm for vehicle following systems, *Industrial Electronics and Applications (ICIEA) 2013 8th IEEE Conference on*, Melbourne, Australia, 19-21 June 2013, pp. 1506-1511.

[4] Vidal R, Shakernia O and Sastry S 2004 Following the flock: distributed formation control with omnidirectional vision-based motion segmentation and visual servoing, *IEEE Robotics & Automation Magazine*, December 2004, vol. 11, no. 4, pp. 14-20.

[5] Krejsa J and Vechet S 2012 Infrared beacons based localization of mobile robot, Electronics And Electrical Engineering, no. 1(117), pp. 17-22.

[6] Ng T C, Ibanez-Guzman J, Shen J, Gong Z, Wang H, and Cheng C 2004 Vehicle following with obstacle avoidance capabilities in natural environments, *Proc. IEEE Int. Conf. Robotics and Automation ICRA '04*, New Orleans, LA, USA, April 2004, vol. 5, pp. 4283-4288.

[7] Shoval S and Borenstein J 2001 Measuring the relative position and orientation between two mobile robots with binaural sonar, *Proceedings of the ANS 9th International Topical Meeting on Robotics and Remote Systems*, Seattle, Washington, USA, 4-8 March 2001.

[8] Hoflinger F and Reindl L M 2012 TDOA based localization using interacting multiple model estimator and ultrasonic transmitter/receiver, *IEEE 9th International Multi-Conference on Systems, Signals and Devices*, Chemnitz, Germany, 20-23 March 2012, vol.1, pp.1063-1069.

[9] Hartikainen J and Sumo S 2011 Optimal filtering with Kalman filters and smoothers, *A Manual for the Matlab toolbox EKF/UKF*, Department of Biomedical Engineering and Computational Science, Aalto University School of Science, Espoo, Finland, August 2011, p.129.

[10] Wang J, Ding W and Wang J 2007 Improving adaptive Kalman filter in GPS/SDINS integration with neural network, *Proceedings of ION GNSS 2007*, Fort Worth, TX, USA, 25-28 September 2007, vol.1, pp.571-579.